INSTITUTE OF PHYSICS PUBLISHING PHYSICS IN MEDICINE AND BIOLOGY

Phys. Med. Biol. **46** (2001) 1997–2007 www.iop.org/Journals/pb PII: S0031-9155(01)23292-8

A variable fluence step clustering and segmentation algorithm for step and shoot IMRT

W Bär, M Alber and F Nüsslin

Abteilung für Medizinische Physik, Radiologische Universitätsklinik, Hoppe-Seyler-Str. 3, 72026 Tübingen, Germany

E-mail: wrbaer@med.uni-tuebingen.de

Received 22 March 2001

Abstract

A step and shoot sequencer was developed that can be integrated into an IMRT optimization algorithm. The method uses non-uniform fluence steps and is adopted to the constraints of an MLC. It consists of a clustering, a smoothing and a segmentation routine. The performance of the algorithm is demonstrated for eight mathematical profiles of differing complexity and two optimized profiles of a clinical prostate case. The results in terms of stability, flexibility, speed and conformity fulfil the criteria for the integration into the optimization concept. The performance of the clustering routine is compared with another previously published one (Bortfeld *et al* 1994 *Int. J. Radiat. Oncol. Biol. Phys.* **28** 723–30) and yields slightly better results in terms of mean and maximum deviation between the optimized and the clustered profile. We discuss the specific attributes of the algorithm concerning its integration into the optimization concept.

1. Introduction

Intensity modulated radiotherapy (IMRT) is being implemented in a growing number of radiotherapy departments and technical solutions continue to be developed as a consequence of the learning process. Of the multitude of IMRT delivery methods available at present, applying multiple fields shaped with a multileaf collimator (MLC) is emerging as a technique of choice. Advantages of the step and shoot method are the relative ease of quality assurance and its close relationship with conventional conformal therapy (Xia and Verhey 1998, De Neve *et al* 1999).

Commonly, a step and shoot treatment plan is generated in two stages: first an inverse treatment planning program computes an optimized intensity modulated fluence weight profile. Then a sequencer transforms the profile into single field segments that have no intensity modulation of their own. The segments are finally delivered in a sequence with the beam turned off while the leaves are moving to form the next segment (Bortfeld *et al* 1994).

The sequencing process of converting the optimized profile into segments has to balance two important strands of the treatment. On one hand, the sequencing should translate the

0031-9155/01/071997+11$30.00

original profile as closely as possible to avoid serious deterioration of the treatment plan. On the other hand, the number of segments should be as small as possible because segment number strongly influences the treatment time (Que 1999). Previously published step and shoot sequencers have dealt with such considerations. Most of them use segments with an integer multiple of a certain number of monitor units (Galvin *et al* 1993, Bortfeld *et al* 1994, Convery and Webb 1998, Xia and Verhey 1998, Siochi 1999), others optimize the segment fluence (De Neve *et al* 1996, Wu *et al* 1999). A detailed study demonstrated that no sequencer has yet been found to be clearly superior in all cases (Que 1999).

In the present paper, we describe a step and shoot sequencer that can be integrated into the optimization process of our treatment planning program. It considers all technical limitations of the MLC. A detailed description of the algorithm and the performance for a variety of mathematical profiles is presented. The tests are also partly performed on a previously published sequencer (Bortfeld *et al* 1994).

2. Methods

Sequencers are commonly implemented after the optimization as an independent part of the treatment planning process. One recently published approach discussed a combination of inverse planning and sequencing in a single optimization loop (Keller-Reichenbecher *et al* 1999). The method did not improve the treatment plans. Nevertheless, integration of the sequencing into the optimization is desirable, because it allows the possibility of optimizing the sequencing with respect to the dose distribution.

The objective of our work was to develop a sequencer that fulfils the conditions for integration into the optimization process. First of all, the sequencer performance has to be sensitive as well as stable. Two slightly different optimized profiles should lead to segments which are slightly but not completely different. Such small changes are likely to happen during the optimization. The sequencing procedure has to be fast, because it will be performed several times during the treatment planning. It should not take longer than a fraction of the time needed for one optimization iteration. It has to deal with all constraints, so that no further adjustments of the resulting segments are necessary after the optimization. An additional goal is the possibility of verification with electronic portal imaging at the beginning of the treatment. The first segment should be the whole field, if this is possible (Webb 1998a). Finally, the integrated sequencer should perform as well as other sequencers when used stand-alone after the optimization.

2.1. Clustering

The result of the optimization process is a quasicontinuous fluence weight profile for every beam orientation. In the clustering stage, the profile is projected onto a piecewise constant fluence weight profile with few levels. From now on, fluence weight is expressed in monitor units (MU). The clustering algorithm works in the following way:

(a) A constant bandwidth b is chosen which specifies the maximum fluence weight deviation of any element between the value before and after the clustering.
(b) Fluence weight elements are grouped together to form clusters. A cluster is composed of one or more elements. The cluster value as one fluence weight level in the clustered profile is calculated as the mean value of all elements that belong to this cluster. An element is added to a cluster if all elements of the resulting cluster are no more than some ϵ apart from the new cluster value. The initial value of ϵ is $b/16$.

(c) If all elements are grouped for a certain ϵ, multiplication by a constant factor increases ϵ. The factor is chosen so that ϵ equals b after 16 iterations. Steps (b) and (c) are repeated until $\epsilon > b$.

Notice that the algorithm ensures that the deviation of any element is equal to or smaller than b, but not that the difference between cluster values is equal to or greater than b. Cluster values are always equal to or greater than the minimum fluence and equal to or smaller than the maximum fluence of the optimized profile. As a consequence, the clustering routine does not exclude elements from the fluence profile by reducing their values to zero. This has to be done by the optimization before the clustering.

The resolution of the profile perpendicular to the direction of leaf motion is the projected leaf width in the isocentric plane, e.g. 1 cm for an Elekta MLC. In the direction of leaf motion, the resolution can be chosen freely, e.g. 0.2 cm. Both dimensions are determined by the optimization.

Technical restrictions of the MLC as described in the following section may mean limiting the minimum segment size in the direction of leaf motion. Additionally, one may want to define additional constraints due to dosimetric concerns about small-sized segments (Zhu and Bjärngard 1994). In our implementation, the clustered profile is smoothed. Peaks (with an MLC constraint) and valleys (with a dosimetric constraint) smaller than the defined limitations are associated with the surrounding cluster. The cluster values are updated after the smoothing. Notice that the maximum fluence deviation of some elements may now exceed b.

Another smoothing routine deals with isolated segments far offset in the direction of leaf motion. If such segments cannot be adequately formed by leaves and backup jaws due to a limited range of movement in the other field half, these segments are extended towards the centre of the field. This kind of correction is not likely to happen very often. Segments will only rarely be offset that far from the centre of the field (e.g. more than 12.5 cm for an Elekta MLC).

2.2. Segmentation

The clustered profile has to be transformed into a series of segments before the treatment. The segmentation has to consider all restrictions such as the minimum field size constraint and the technical limitations of the MLC being used for treatment. In what follows, an adoption for an Elekta MLC is discussed. A design for other MLCs is possible if the types of limitations are the same.

Regions of non-zero fluence that are separated by regions of zero fluence in the direction of leaf motion cannot be irradiated at the same time (see part (i) of figure 1). Specifically for an Elekta MLC, one has to consider that opposing leaves and x-jaws (backup-jaws) cannot completely close (minimum gap constraint), a leaf from one leaf bank cannot pass an adjacent leaf of the other bank (interdigitation constraint), leaves and x-jaws have a limited range of travel into the other field half and y-jaws cannot pass the centre of the field (maximum overtravel constraints).

Henceforth, leaf movement is in the x direction, leaf pairs are labelled in the y direction and z denotes the fluence. The algorithm works in the following way (see also figure 1 for illustration):

(a) The segmentation starts with as many segments as there are clusters. The first segment consists of all non-zero elements, the second of all non-zero elements but those with the minimum fluence weight. This scheme is repeated, so that the last segment is composed of all elements with a maximum fluence value. The minimum fluence value of every segment is assigned to it as monitor units.

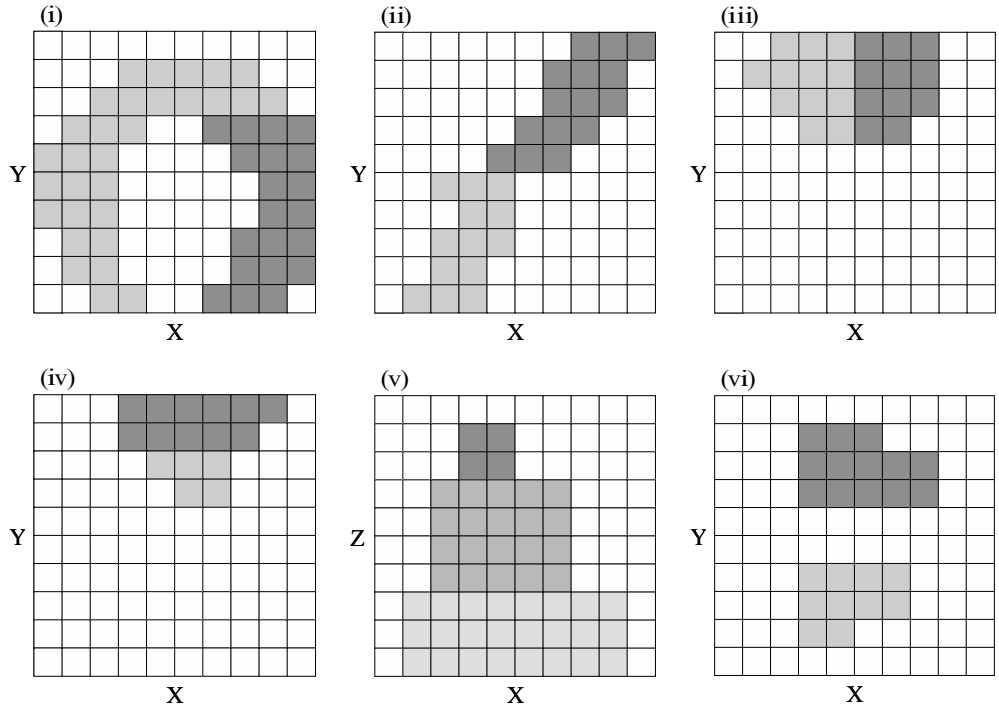

Figure 1. Examples of the performance of the segmentation algorithm. White squares are zero elements, grey squares non-zero elements and grey scales illustrate the different segments. An exception is part (v), where fluence is plotted against position. (i) Horizontal cut due to in-field fluence minima in the direction of leaf motion. (ii) Horizontal cut due to violation of the interdigitation constraint. (iii) Vertical cut to be able to shield the space between the segment and the field centre. (iv) Horizontal cut because a vertical cut would violate the minimum gap constraint. (v) Monitor units for three segments as height of the relevant quadrangle. (vi) Segments that can be merged to form a new segment.

(b) If a segment has in-field fluence minima in the direction of leaf motion, the segment is split along a horizontal line (see part (i) of figure 1). The procedure is repeated for all segments until none of the resulting segments has any of those minima.

(c) If a segment violates the interdigitation constraint, the segment is split along a horizontal line as demonstrated in part (ii) of figure 1. Step by step, all such violations are erased for every segment.

(d) If a segment is completely in the lower or upper half, the space between the segment and the centre of the field has to be exclusively shielded by the leaves due to the maximum overtravel constraint of the y-jaws. In this region, either the left leaves have to be moved under the right x-jaw or the right leaves have to be moved under the left x-jaw. If this is not possible without violating any of the constraints, the segment is split along a vertical line if no additional constraint violations are introduced (see part (iii) of figure 1). Otherwise, the split is aligned horizontally (see part (iv) of figure 1). After these checks and eventual splits have been performed for every segment, all the resulting segments are usable for treatment.

(e) As a consequence of the algorithm, there may be some segments with an identical shape and some segments that are part of others. The monitor units of those segments are updated (see part (v) of figure 1 for an example) and henceforth unnecessary segments are erased.

(f) Segments that can be treated together are merged to form a new segment (see part (vi) of figure 1). This will only happen if both segments have the same monitor units and the resulting segment does not violate any constraint.

The combination of clustering, smoothing and segmentation guarantees that the clustered profile is transformable into segments without further adjustments. The superposition of all segments exactly reproduces the clustered profile after smoothing.

The algorithm does not avoid the tongue-and-groove effect. Recent investigations showed in general no clinical significance of the tongue-and-groove effect for IMRT treatments with five or more beam orientations (Deng *et al* 2001). One aim is to develop a segmentation routine that can decide from case to case whether to avoid the tongue-and-groove effect or not.

3. Results

The performance characteristics of the sequencer were analysed for a specific implementation of the algorithm for an Elekta MLC with 40 leaf pairs. The minimum gap and the interdigitation constraint were set to 1 cm. The maximum overtravel of leaves and x-jaws was 12.5 cm. (For further details of the Elekta MLC see Jordan and Williams (1994).) The calculated resolution was 0.2 cm in the direction of leaf motion and 1 cm perpendicular to that. These restrictions led to a minimum field size constraint of 1 cm in both directions.

We analysed the sequencing for eight mathematical profiles of varying complexity, four of them 2D profiles, the others 3D profiles (see figure 2). The size of the calculation grid was 61 times 40, which led to field dimensions of 13.2 cm in the direction of leaf motion and 40 cm perpendicular to that. The smooth analytical profiles modelled the optimized profiles of the inverse treatment planning program Hyperion which are also smoothed (Alber *et al* 2000, Alber and Nüsslin 2000). All profiles were normalized so that the maximum weight was always 100 MU and the minimum weight 9.1 MU. Notice that the clustering is independent of the size and scale of the calculation grid. As a consequence, the results of the clustering for other grid sizes and scales are similar. However, the finer the spatial modulation of the profiles, the more the smoothing routines modify the clustered profiles.

Additionally, two fields with a beam orientation of 72° and 288° for a five field prostate case were optimized with our inverse treatment planning program and the sequencing was analysed. Both profiles were normalized to a maximum weight of 100 MU.

3.1. Clustering

The clustering was analysed for all eight analytical profiles with a bandwidth equal to, twice and four times the minimum weight of 9.1 MU. The optimized prostate profiles were clustered with a bandwidth half, equal to and twice the respective minimum fluence. We investigated the mean squared deviation between the original and the clustered profile

$$\mathrm{rms} = \sqrt{\frac{1}{n}\sum_{i=1}^{n}(\Phi_{\mathrm{or},i} - \Phi_{\mathrm{cl},i})^2} \tag{1}$$

where n is the number of fluence weight elements, $\Phi_{\mathrm{or},i}$ the weight of the ith element of the original profile and $\Phi_{\mathrm{cl},i}$ the weight of the ith element of the clustered profile. Other values of interest are the maximum deviation between the original and clustered profile of a single element, in what follows named 'max', and the time needed for the clustering process.

The method was compared with a previously published one (Bortfeld *et al* 1994), henceforward called the 'Bortfeld method'. In short, this algorithm projects the original profile

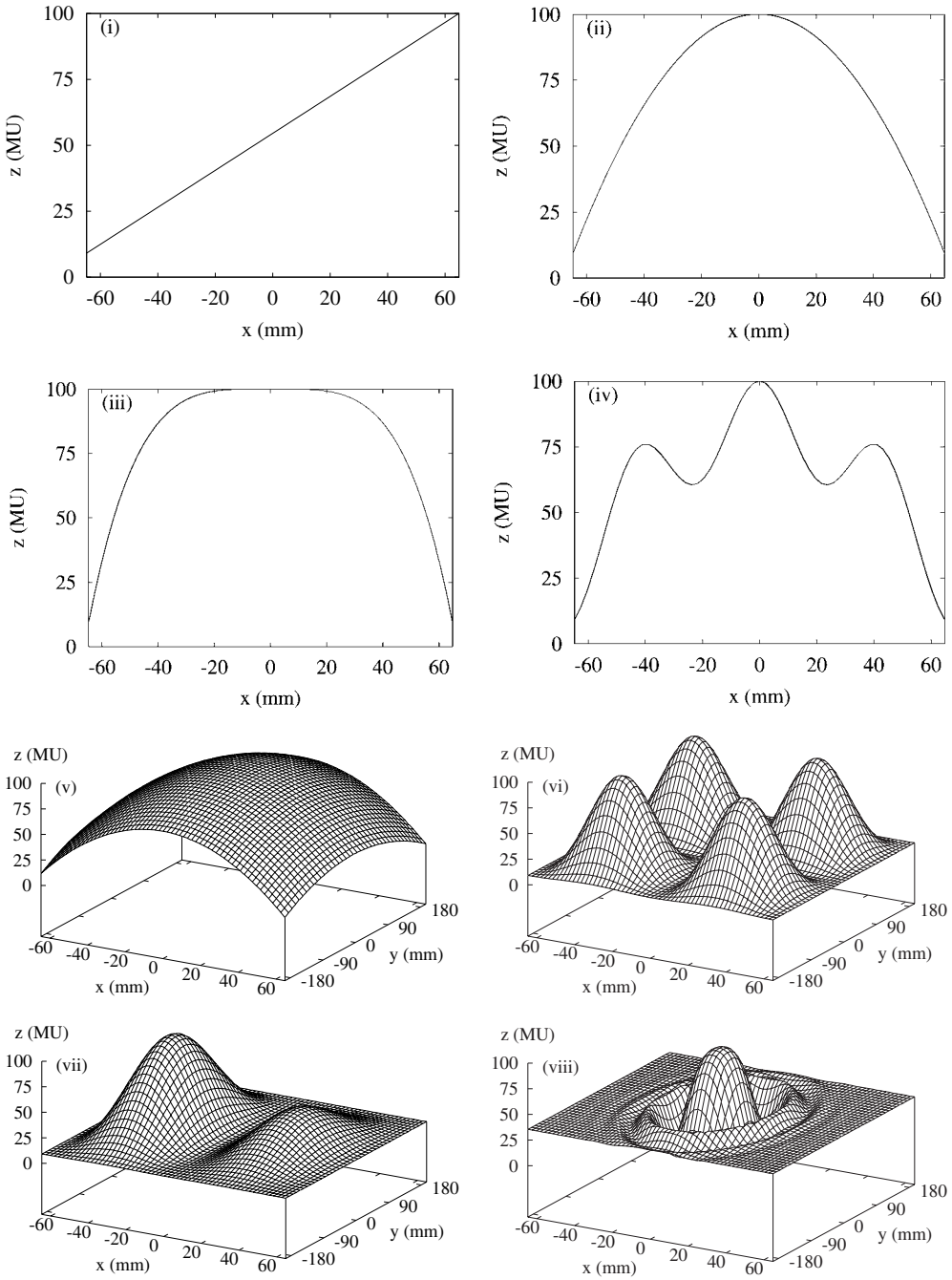

Figure 2. Mathematical profiles to test the performance of the sequencer. Notice that a_1 is used for the left peak and a_2 for the right peak of profile (vii): (i) $z = x + \text{const.}$ (ii) $z = -x^2 + \text{const.}$ (iii) $z = -x^4 + \text{const.}$ (iv) $z = -0.002x^2 + \cos^2(0.05\pi|x|) + \text{const.}$ (v) $z = -(x^2 + y^2) + \text{const.}$ (vi) $z = \sin^2(0.033\pi|x|)\sin^2(0.05\pi|y|) + \text{const.}$ (vii) $z = a_i \sin^2(0.033\pi|x|)\cos^2(0.025\pi|y|) + \text{const.}$ $(a_1 = 7/3a_2)$. (viii) $z = \cos[0.033(x^2 + y^2)]/\exp[0.01(x^2 + y^2)] + \text{const.}$

Table 1. Analysis of the clustering and segmentation for 10 profiles with three different bandwidths. Listed are the resulting number of clusters and segments and rms and max for our clustering method (labelled with the subscript 1) and for the Bortfeld method (labelled as with the subscript 2). Bandwidth, rms and max have MU as their unit.

Profile	Bandwidth	Clusters	Segments	rms_1	rms_2	max_1	max_2
1	36.4	3	3	9.7	9.4	18.2	16.7
	18.2	4	4	6.7	7.1	11.4	12.5
	9.1	8	8	3.4	3.7	5.3	6.3
2	36.4	3	3	9.6	9.8	21.2	19.4
	18.2	5	4	5.4	6.1	10.9	11.8
	9.1	8	8	3.3	3.8	6.6	7.2
3	36.4	3	3	8.0	9.6	20.9	21.4
	18.2	4	4	5.9	7.0	14.0	14.3
	9.1	9	9	2.6	3.4	7.3	7.4
4	36.4	2	2	12.5	12.5	26.2	25.0
	18.2	4	4	6.3	7.5	13.3	14.2
	9.1	7	9	3.4	4.2	8.0	7.1
5	36.4	3	3	8.6	9.0	21.9	16.7
	18.2	4	4	7.0	7.2	15.4	12.5
	9.1	8	8	3.7	3.6	8.7	6.3
6	36.4	3	11	10.2	8.1	25.1	16.7
	18.2	4	15	6.7	5.9	14.9	12.5
	9.1	7	31	3.5	3.8	9.0	8.6
7	36.4	3	4	6.9	7.7	20.4	20.0
	18.2	4	5	5.6	5.6	15.5	12.5
	9.1	9	12	2.9	3.5	7.1	6.7
8	36.4	3	3	7.0	10.2	24.9	26.7
	18.2	4	6	3.8	4.0	13.2	12.5
	9.1	8	17	1.9	2.8	7.4	8.7
72°	37.6	3	3	7.9	10.0	22.3	23.3
	18.8	5	5	4.9	6.8	14.3	12.0
	9.4	8	8	3.1	4.2	7.5	7.5
288°	46.2	3	2	7.9	10.2	21.7	23.3
	23.0	4	4	5.1	8.8	18.2	15.0
	11.5	7	7	3.8	5.1	10.9	8.6

onto a profile of equally spaced fluence levels. The distance between adjacent levels and a offset which determines the position of the first fluence level is chosen before the clustering (for details see Bortfeld *et al* 1994).

The maximum fluence value which resulted from our method was divided by the number of clusters and determined the distance between fluence levels for the Bortfeld method, which was accomplished afterwards for 11 offsets (0.0, 0.1, . . . , 1.0 times the level distance). The offset which resulted in the minimum rms was chosen for comparison with our method. Notice that an offset of 0.5 times the level distance guarantees the smallest theoretically possible max (equal to or smaller than 0.5 times the difference in fluence between adjacent levels), but not necessarily the minimum rms. The results of both methods in terms of rms and max are summarized in table 1.

Table 2. Results of smoothing and updating of the cluster values for all 10 cases that violated the minimum gap or the minimum field-size, constraint after clustering. Subscript 1 denotes the values after clustering, subscript 2 after smoothing and subscript 3 after updating. Bandwidth, rms and max have MU as their unit.

profile	bandwidth	rms_1	rms_2	rms_3	max_1	max_2	max_3
7	9.1	2.91	2.94	2.93	7.13	7.83	7.13
8	36.4	7.03	7.06	7.06	24.88	24.88	24.93
8	18.2	3.77	5.47	5.42	13.21	26.69	25.98
8	9.1	1.92	3.86	3.65	7.36	25.84	26.07
72°	9.4	3.1	5.5	5.3	7.5	35.7	33.2
72°	18.8	4.9	6.1	6.0	14.3	25.8	24.7
72°	37.6	7.9	8.0	8.0	22.3	22.3	22.3
288°	11.5	3.8	5.0	5.0	10.9	23.6	22.9
288°	23.0	5.1	6.0	6.0	18.2	22.4	21.6
288°	46.0	7.9	8.0	8.0	21.7	21.7	22.0

All 30 cases resulted in 2 to 9 clusters. These numbers are reasonable for IMRT treatments with about 30 to 70 segments divided into five or more beam orientations (see the resulting number of segments in the same table). The rms of our clustering spanned from 1.9 MU to 12.5 MU with a mean value of 5.9 MU, the rms of the Bortfeld method from 2.8 MU to 12.5 MU with a mean value of 6.7 MU. The max of our method varied between 5.3 MU and 26.2 MU with a mean value of 14.5 MU, the max of the Bortfeld method varied between 6.3 MU and 26.7 MU with a mean value of 13.8 MU. Notice that the value of rms is more meaningful than the value of max, because rms is the parameter that was optimized by both clustering algorithms. Max is controlled by bandwidth or distance between adjacent fluence levels, which are both chosen before the clustering. As a consequence, the clustering with our method led on average to slightly better results than those of the Bortfeld method. Our algorithm needed between 0.45 s and 0.63 s for any profile on a 900 MHz personal computer.

No profile violated the maximum overtravel constraint after the clustering, but some profiles violated the minimum gap or the minimum segment-size constraint. The subsequent smoothing routine erased the relevant peaks and valleys so that all violations were eliminated. Afterwards, new cluster values were calculated in the aforementioned fashion. The rms and max before the smoothing, after smoothing and after smoothing and cluster updating are shown in table 2 for all profiles that violated any constraint after the clustering. The influence of smoothing depended strongly on the exact profile and increased the rms to up to about 100%; the max was affected even more strongly. The subsequent update of the cluster values reduced the rms slightly (in some cases this is not visible in table 2 due to rounding). It seems to be likely that a more sophisticated method of smoothing could lead to better results.

3.2. Segmentation

The segmentation algorithm was applied to the clustered profiles. The resulting number of segments is listed in table 1. Profiles without in-field minima in the direction of leaf motion mostly needed only one segment per cluster, whereas profiles with existing in-field minima after clustering and smoothing required additional segments. As an example see figure 3, where profile 4 with four clusters without an in-field minimum led to four segments, whereas the same profile with seven clusters and two in-field minima resulted in nine segments. A statistical measure for the quality of the segmentation is the segment to cluster ratio. The lower boundary of the ratio is fixed by the complexity of the profile. Centred profiles without

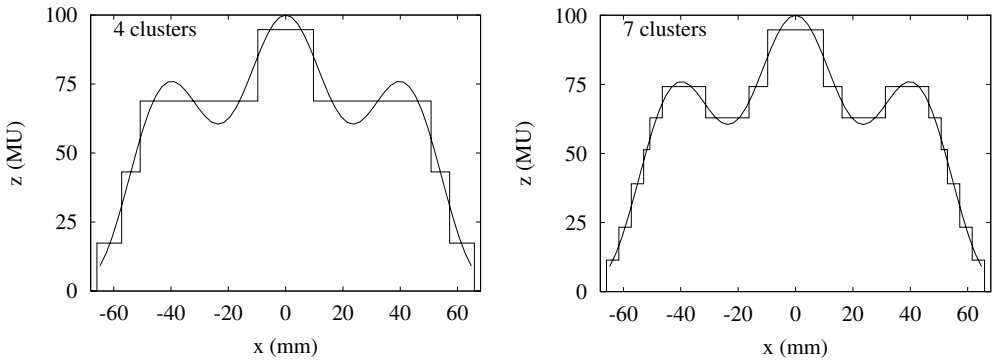

Figure 3. Optimized and clustered profile with four and seven clusters respectively. The clustered profile on the left has no in-field minima, every cluster is a single segment. The clustered profile on the right has two in-field minima, seven clusters lead to nine segments.

in-field minima mostly have a minimum ratio of 1. For each profile, we estimated the minimum ratio through considerations about in-field minima, interdigitation violations and offsets from the centre of the field. Adequate segmentation algorithms should lead to ratios equal to or barely greater than the minimum one, otherwise unnecessary segments have been created. For all profiles apart from profile 6 the ratio was around one to two and therefore equal to or close to the minimum. Profile 6 was a complicated case for the constraints used. There was an in-field fluence minimum for almost every leaf pair and all four peaks were offset from the centre of the field in the y-direction, thus leading to maximum overtravel problems of the y-jaws. As a consequence, the resulting as well as the minimum ratios were quite big. Another special case was the 288° profile with a bandwidth of 46.2 MU, where the smoothing reduced the number of clusters from three to two which finally led to two segments. The whole process was computed in about 0.02 s to 0.03 s.

Segmentation and smoothing after clustering were not performed for the Bortfeld method, because it is not applicable to the Elekta MLC constraints without major changes (Convery and Webb 1998). However, the investigation of resulting and minimum segment to cluster ratios showed satisfying outcomes for our algorithm.

4. Discussion

The integration of the sequencer into an optimization concept requires features which are ensured by the combination of clustering, smoothing and segmentation:

- The clustering is stable as well as sensitive. The variable fluence step method allows every single fluence weight element to influence the cluster values and, consequently, the whole clustered profile in a moderate fashion. This is not the case for the 'more discrete' Bortfeld method, where a variety of slightly different optimized profiles may result in the same clustered profile as a consequence of the fixed fluence pitch.
- The whole algorithm is sufficiently fast to be just a fraction of one optimization iteration.
- The sequencer considers all technical and dosimetric restrictions.
- Verification through electronic portal imaging with the largest segment first is possible, because the size of this segment is maximized. Obviously, some profiles will not allow a segment which consists of the whole field due to technical limitations (e.g. profile (vi) in figure 2).

- The conformity between the original and the clustered profile is on average slightly better than with the Bortfeld method. The segmentation performance shows no tendency to create unnecessary segments.

The sequencing method differs in one major aspect from most of the previously published ones (Galvin *et al* 1993, Bortfeld *et al* 1994, Convery and Webb 1998, Xia and Verhey 1998, Siochi 1999) as the clustering uses non-uniform fluence steps. Additionally, the segmentation is not performed according to the 'sliding-window' technique, where every leaf will only move in one direction during the irradiation of all segments from one beam orientation (Convery and Webb 1998).

The use of variable instead of uniform fluence steps introduces an additional degree of freedom for the clustering. It is obvious that this should on average result in equal or better conformity between the optimized and clustered profiles for a fixed number of fluence levels. When discussing the clustering alone, the only argument for the use of uniform steps would be that the better conformity of variable steps may not be significant (Evans *et al* 1997). This statement may be true for a large number of clusters, but remains questionable apart from that, as for example the clustering of both clinical cases resulted in significantly better conformity when performed with our clustering method (see table 1). Generally, high clinical applicability is chained to only a few segments or clusters.

The sliding-window method combined with uniform fluence step clustering offers a great number of possibilities to decompose a clustered profile into segments (Webb 1998a, b), this way being well suited to minimize the number of segments and to maximize the monitor unit efficiency (Que 1999). Additionally, it is closely related to the 'dMLC' technique, where the irradiation is not interrupted while the leaves are moving (Convery and Webb 1998). On the other hand, verification with electronic portal imaging is not possible for a pure sliding-window treatment. A compromise such as the suggested 'forced-baseline' technique reduces the aforementioned benefits (Webb 1998a).

Inverse treatment planning with the integrated sequencer offers new possibilities. After the optimization of the fluence profile, the sequencer generates segments which can be used for further optimization. One possibility is the optimization of the segment weights and shapes by evaluating an objective function taking the segments into consideration. Another is the exclusive optimization of the segment weight with another objective function. Details of these methods will be the subject of a forthcoming paper (Alber and Nüsslin 2001).

5. Conclusion

A step and shoot sequencer was developed for integration into an IMRT optimization algorithm. It uses a clustering algorithm with non-uniform fluence steps and takes account of the limitations of an Elekta-MLC. The segmentation leads to a series of segments that offer the possibility to do verification through electronic portal imaging with the first segment.

A performance analysis demonstrated the sequencing characteristics for several mathematical profiles of varying complexity, partly in comparison with a previously published sequencer (Bortfeld *et al* 1994). The results in terms of stability, sensitivity, speed and conformity are sufficient for the integration into the optimization concept. The clustering showed on average slightly smaller mean deviations between clustered and optimized profiles than with the Bortfeld method.

Acknowledgments

We are indebted to the William Beaumont Hospital, Royal Oak, for the provision of a sequencing code and the clinical test cases. The segmentation described here refines some concepts of this source. Our work was supported by the Deutsche Krebshilfe e.V.

References

Alber M and Nüsslin F 2000 Intensity modulated photon beams subject to a minimal surface smoothing constraint *Phys. Med. Biol.* **45** N49–N52

——2001 IMRT optimization under constraints for static and dynamic MLC delivery *Phys. Med. Biol.* submitted

Alber M, Birkner M, Laub W and Nüsslin F 2000 Hyperion—an integrated IMRT planning tool *Proc. 13th Int. Conf. on Computers in Radiotherapy* pp 46–8

Bortfeld T R, Kahler D L, Waldron T J and Boyer A L 1994 X-ray field compensation with multileaf collimators *Int. J. Radiat. Oncol. Biol. Phys.* **28** 723–30

Convery D J and Webb S 1998 Generation of discrete beam-intensity modulation by dynamic multileaf collimation under minimum leaf separation constraints *Phys. Med. Biol.* **43** 2521–38

De Neve W, De Gersem W, Derycke S, De Meerleer G, Moerman M, Bate M-T, Van Duyse B, Vakaet L, De Deene Y, Mersseman B and De Waeter C 1999 Clinical delivery of intensity modulated conformal radiotherapy for relapsed or second-primary head and neck cancer using a multileaf collimator with dynamic control *Radiother. Oncol.* **50** 301–14

De Neve W, De Wagter C, De Jaeger K, Thienpont M, Colle C, Derycke S and Schelfhout J 1996 Planning and delivering high doses to targets surrounding the spinal cord at the lower neck and upper mediastinal levels: static beam-segmentation technique executed with a multileaf collimator *Radiother. Oncol.* **40** 271-79

Deng J, Pawlicki T, Chen Y, Li J, Jiang, S B and Ma C-M 2001 The MLC tongue-and-groove effect on IMRT dose distributions *Phys. Med. Biol.* **46** 1039–60

Evans P M, Hansen V N and Swindell W 1997 The optimum intensities for multiple static multileaf collimator field compensation *Med. Phys.* **24** 1147–56

Galvin J M, Chen X-G and Smith R M 1993 Combining multileaf fields to modulate fluence distributions *Int. J. Radiat. Oncol. Biol. Phys.* **27** 697–705

Jordan T J and Williams P C 1994 The design and performance characteristics of a multileaf collimator *Phys. Med. Biol.* **39** 231–51

Keller-Reichenbecher M-A, Bortfeld T, Levegrün S, Stein J, Preiser K and Schlegel W 1999 Intensity modulation with the 'step and shoot' technique using a commercial MLC: a planning study *Int. J. Rad. Oncol. Biol. Phys.* **45** 1315-1324

Que W 1999 Comparison of algorithms for multileaf collimator field segmentation *Med. Phys.* **26** 2390-6

Siochi R A C 1999 Minimizing static intensity modulation delivery time using an intensity solid paradigm *Int. J. Radiat. Oncol. Biol. Phys.* **43** 671–80

Webb S 1998a Configuration options for intensity-modulated radiation therapy using multiple static fields shaped by a multileaf collimator *Phys. Med. Biol.* **43** 241–60

——1998b Configuration options for intensity-modulated radiation therapy using multiple static fields shaped by a multileaf collimator. II: Constraints and limitations on 2D modulation *Phys. Med. Biol.* **43** 1481–95

Wu Y, Yan D, Sharpe M, Miller B and Wong J 1999 A method of generating multiple static fields and delivering intensity modulated radiotherapy *Med. Phys.* **26** 1137

Xia P and Verhey L J 1998 Multileaf collimator leaf sequencing algorithm for intensity modulated beams with multiple static segments *Med. Phys.* **25** 1424–34

Zhu T C and Bjärngard B E 1994 The head-scatter factor for small field sizes *Med. Phys.* **21** 65–8